

Zeolite NaA Membranes Supported on α -alumina Cylindrical Tubes

Masakazu Kondo, Tadafumi Yamamura, Etsuo Sugimoto and Hidetoshi Kita*

Mitsui Engineering & Shipbuilding Co. Ltd., 3-1-1, Tama, Tamano, Okayama 706-865, Japan

Fax: 81-863-23-2777, e-mail: kondomas@mes.co.jp

* Faculty of Engineering, Yamaguchi University, Tokiwadai, Ube Yamaguchi 755-8611, Japan

Fax: 81-836-85-9601, e-mail: kita@po.cc.yamaguchi-u.ac.jp

Zeolite NaA membranes were prepared on the surfaces of α -alumina cylindrical supports using the hydrothermal synthesis. Regardless of the porosity size of the α -alumina support, the zeolite membranes consisted of three layers. Compared with the previous membrane, which was prepared on mullite support, the zeolite crystals layer was thicker and the intermediate layer was thinner. Grain boundary clearance (non-zeolite pore) size of the membrane was evaluated by permoporometry. Average Kelvin diameters, which were defined as the diameters at nitrogen permeance of 50 %, were at ca. 1.8 nm Kelvin diameters regardless of the porosity size of the support. The maximum value of the pore size distribution of the zeolite membranes was at ca. 1.6 nm Kelvin diameters regardless of the porosity size of the support, and only its value increased with the increase in the porosity size of the support. The membrane performance in pervaporation (PV) increased with the increase in the porosity size of the support. For industrial application of the membranes, the support of 37.6 % porosity was adopted from economic standpoint. The membrane was ca. 1.2 times as high performance as the previous membrane. A high separation mechanism of PV and vapor permeation (VP) based on the capillary condensation (or pore-filling) of water in the non-zeolite pores and the blocking of other molecules from entering the pores was proposed.

Key words: Pervaporation, Zeolite NaA membrane, Alumina support, Dehydration, Permoporometry

1. INTRODUCTION

Pervaporation (PV) is an attractive means as an effective and energy-efficient technique for the dehydration of water/organic mixtures [1]. Zeolite membranes offered significant potential for PV agent with high separation factor and permeation flux together with high chemical and thermal stability. In order to purify isopropanol (IPA) from cleaning process in industries such as precision machinery and electronics, and to dehydrate ethanol (EtOH) used in food industry, PV or vapor permeation (VP) equipment using each of NaA-type and T-type zeolite membranes has been used practically [2,3]. In these membranes, mullite supports were used for the cost reduction, though PV performance of these membranes was lower than one of the zeolite membranes prepared on α -alumina supports. It has been reported that the membrane performance increases with the increase in the alumina content in the mullite support [4]. Structure and chemistry of support materials play an important role in zeolite membrane formation and have a significant influence on the separation property of the membrane material [5].

In comparison with the mullite support cost, the high cost of α -alumina support occurs by the adoption of the uniform grain size. By not sticking to the adoption of the uniform grain size, it was found that the cost of α -alumina support was cut down. However, the relationship between

membrane performance and physical properties of α -alumina support has not been clarified yet.

Grain boundary clearance (non-zeolite pore) size of zeolite NaA membranes and PV properties for IPA/water mixture were examined using the α -alumina supports with different porosity size, of which the average surface roughness and average pore diameter were almost identical.

In this paper, using the computer-controlled nanopermoporometry [6], the non-zeolite pore size of the zeolite membranes was measured. Moreover, the relationship between the membrane performance and porosity size of the support was examined in PV. For industrial application of the membranes, supports were discussed from economic standpoint. PV and VP performance of the membrane used practically were examined with organic solvent/water mixtures at various temperatures.

2. EXPERIMENTAL

2.1 Membrane preparation

The synthesis method for the zeolite NaA membrane was that of Kita et al. [7-9], and the detailed procedure was described elsewhere [9]. The molar composition of the starting gel was $\text{Al}_2\text{O}_3:\text{SiO}_2:\text{Na}_2\text{O}:\text{H}_2\text{O}=1:2:2:120$. Crystallization was carried out for 3.5 hours at 373 K. Several α -alumina supports with different porosity size were used in this study. The physical properties

on their supports (supplied by Nikkato Corp.) are summarized in Table 1.

Table 1. Physical property and purchase price of supports

Name	Material	Size od.(mm) × id.(mm) × L.(mm)	Porosity %	Surface Roughness μm^{**}	Price yen/tube
PM	Mullite	$\phi 12 \times 9 \times 800\text{L}$	43.8	1.3	1,050
Type-E	α -Alumina	$\phi 12 \times 9 \times 800\text{L}$	36.2	0.4	1,050
Type-F	α -Alumina	$\phi 12 \times 9 \times 800\text{L}$	37.6	0.5	1,050
Type-G	α -Alumina	$\phi 12 \times 9 \times 800\text{L}$	43.1	0.5	Price rises with porosity size
Type-H	α -Alumina	$\phi 12 \times 9 \times 800\text{L}$	45.4	0.6	

** Surface Roughness Measuring Method ; JIS(B-0601)

In this Table, the physical property of previous mullite support has also been described.

2.2 Nanopermporometry characterization of zeolite membranes

Non-zeolite pore size of the zeolite membranes was measured using nanopermporometry [6]. Nitrogen was used as a non-condensable gas, and the liquid used as a condensable vapor was water. The zeolite membranes were heated at 473 K in the vacuum to remove any adsorbates, and then, they were set in the equipment. For the calculation of Kelvin diameter based on Eq. 1, complete wetting, i.e. contact angle $\theta = 0$, was assumed.

$$RT \ln(p/p_{\text{sat}}) = -v2\sigma \cos\theta / r_p \quad (1)$$

Where p is water vapor pressure in the feed nitrogen gas and p_{sat} is the saturated vapor pressure, σ is the surface tension between water and nitrogen, v is the molar volume of water, and r_p is the capillary radius.

Under the studied experimental conditions, the mean free path λ of nitrogen is much larger than the pore (zeolite pore and non-zeolite pore) size of the membrane (λ is about 35 nm at 2 atm and 293 K). The permeation of nitrogen through these pores of the membrane is governed by the Knudsen diffusion mechanism [10]. Thus the pore size distribution of the membrane was calculated from the nitrogen permeance J by Eq. 2.

$$f(r) = -3l\tau / (2rA) \cdot \sqrt{\pi MRT / 8} \cdot dJ/dr \quad (2)$$

Where A is the pore area, $f(r)$ is the pore size distribution function, with a physical meaning of the number of the active pores with radius from r to $r+dr$ per unit membrane area, l is the thickness of top layer on the support, τ is the top layer tortuosity, M is the molecular weight of nitrogen, T is the membrane temperature.

When the measurement condition is constant, the pore size distribution is correspondent with Eq. 3, because Eq. 2 shows only the relation between pore size change and nitrogen permeance change.

$$-dJ/dr = f(r) \cdot 2 / (3l\tau) \cdot \sqrt{8\pi MRT} \cdot r^3 = f'(r) \quad (3)$$

In this study, Eq. 3 was used to examine the effect on the pore size distribution of zeolite membranes by the porosity size of the support.

3. RESULTS AND DISCUSSION

3.1 Characterization of zeolite membranes

To discuss the difference of membrane aspect, the morphologies of the zeolite NaA membranes on the α -alumina supports in Table 1 were observed by SEM. The surfaces of these alumina supports were rather rough and larger pores of several μm in size were present in the surfaces, though their surfaces were smoother than that of mullite support.

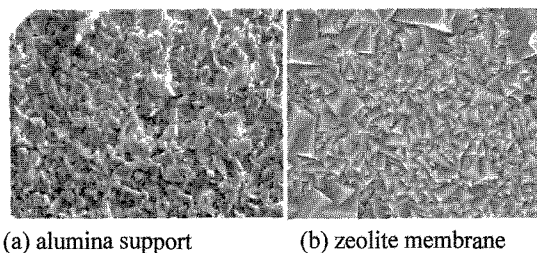


Fig. 1. SEM micrographs of surfaces

Figure 1 shows SEM photographs of the surface of the alumina support with 37.6 % porosity and the surface of the membrane on its support. Regardless of the porosity size of the alumina support, the surface of these supports was completely covered with zeolite NaA crystals, 1 ~ 4 μm in size, and the packing of the crystals was very dense. No space (cavity) between the crystal particles was found by the SEM observation. Regardless of the porosity size of the alumina support, the zeolite membranes consisted of three layers. Compared with the previous membrane, which was prepared on mullite support, the zeolite crystals layer was thicker and the intermediate layer was thinner. The dense zeolite-crystals layer of these membranes was about 15 μm thicker than one of the previous membrane (ca. 10 μm). In all these membranes as well as the previous membrane, the crystals were randomly arranged.

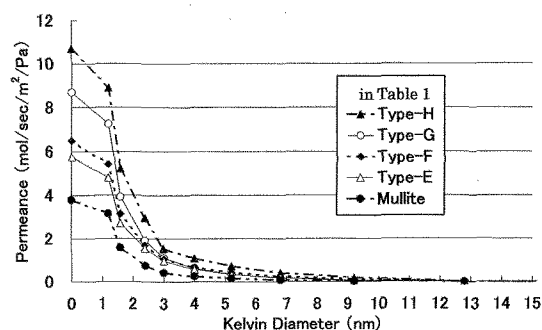


Fig. 2. Nitrogen permeance as a function of Kelvin diameter

Non-zeolite pore size of all membranes was measured using permporometry. The nitrogen permeance is shown in Fig. 2 as a function of Kelvin diameter calculated by Eq. 1 without correction of the adsorption thickness of water vapor. The non-zeolite pore size distribution calculated from nitrogen permeance data in Fig. 2

using Eq. 3 is shown in Fig. 3. It should be noted that the Kelvin equation loses physical meaning for pore diameters of less than 2 nm. Though the present method cannot accurately evaluate the nanoporometry characterization of zeolite membranes, it is an effective method for the comparison of the non-zeolite pore distribution of each membrane.

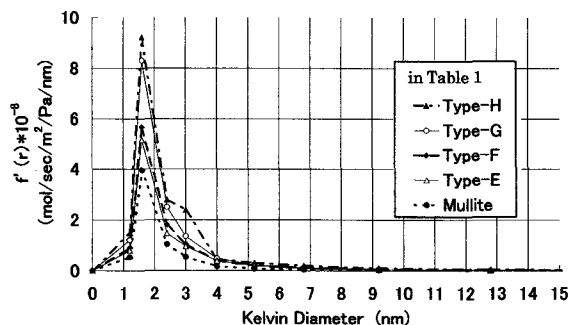


Fig. 3. Non-zeolite pore size distribution of zeolite membranes calculated from nitrogen permeance data

Average Kelvin diameters, which were defined as the diameters of nitrogen permeance of 50 %, were at ca. 1.8 nm Kelvin diameters regardless of the porosity size of the support. The maximum value of the non-zeolite pore distribution of zeolite membranes was at ca. 1.6 nm Kelvin diameter regardless of the porosity size of the support, and only its value increased with the increase in the porosity size of the support. Due to the blocking effect of nitrogen permeation by condensed water, no nitrogen permeation was observed when p/p_{sat} was larger than 0.7.

Table 2. Maximum value of $f'(r)$ and permeation flux

Name	Material	Porosity %	$f'(r)$ mol/sec/m ² /Pa	Flux* kg/h/m ²
PM	Mullite	43.8	3.95	4.58
Type-E	α -Alumina	36.2	5.17	5.01
Type-F	α -Alumina	37.6	5.67	5.33
Type-G	α -Alumina	43.1	8.30	6.37
Type-H	α -Alumina	45.4	9.23	7.67

* PV with 95 wt% IPA at 383 K

The maximum values of the non-zeolite pore distribution of these membranes are compared in Table 2. It seems that almost same sizes of non-zeolite pore are formed in the zeolite membranes prepared under the similar synthesis condition. These results suggest that the number of the non-zeolite pore with the maximum value, which contributes to nitrogen permeance, is dependent on the porosity size of the support.

3.2 PV and VP properties

In order to investigate the effect of the porosity size of the supports on permselectivity, PV experiments were carried out at 383 K using IPA/water mixture with water concentration of 5 wt%. Effect of the size of the support porosity on PV performance of zeolite membranes is shown

in Table 2. Regardless of the porosity size of the supports, the membranes were highly water permeable for IPA solution and displayed extremely high permeation fluxes and separations. The membrane performance in PV increased with the increase in the porosity size of the support. For industrial application of the membrane, the support choice must be determined primarily by economic standpoint.

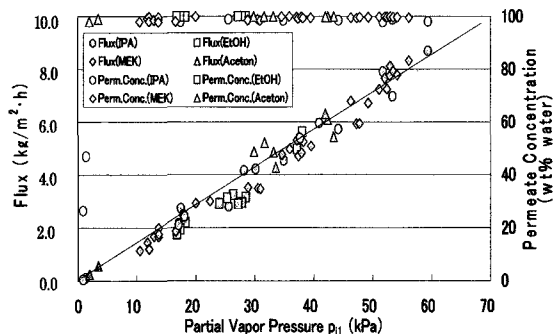


Fig. 4. Effect of partial vapor pressure of feed on permeation flux (α -alumina support of 37.6 % porosity)

Purchase price of supports under porosity size of 37.6 % is the same as shown in Table 1. However, price of supports of >40 % porosity rises with porosity size. Therefore, the zeolite membrane on the support of 37.6 % porosity was used practically. This membrane was ca. 1.2 times as high performance as the previous membrane. The effects of the partial vapor pressure of feed side on the water flux in PV and VP are shown in Fig. 4. The permeation flux of the water in all solvents varied in proportion to partial vapor pressure of feed side regardless of operation condition in PV and VP. The gradient was almost constant without being dependent on nature and concentration of the solvent. The permeation was almost the water and the separation factor was over 10000.

3.3 Permeation and separation mechanism

In this study, permeation and separation mechanism of PV and VP was discussed using gas diffusion model. In general, gas diffusion in microporous media is described in terms of surface diffusion and activated gas translation diffusion. It seems that the mass transport in zeolite NaA membrane can be expressed by the description of Broeke et al. [11], because the membrane is a microporous material. We have extended their description and we assume that both of the surface diffusion $J_{s,i}$ in zeolite pore and the activated gas translation diffusion $J_{GT,i}$ in non-zeolite pore contribute to the overall mass transport $J_{\text{total},i}$ for species i in the mixture through the membrane in PV and VP. Therefore, the relative area ε of zeolite pore and non-zeolite pore must be considered, as the following Eq. 4.

$$J_{\text{total},i} = (\varepsilon \cdot J_{s,i} + (1-\varepsilon) \cdot J_{GT,i}) \cdot \Phi \\ = (\varepsilon \cdot \rho q_{i,\text{sat}} D_i^{\circ}(0) \cdot 1/(1-\theta) \cdot \exp(-E_{s,i}/RT) \cdot d\theta/dx \\ + (1-\varepsilon) \cdot \lambda/z \cdot \sqrt{8/(\pi MRT)} \cdot \exp(-E_{GT,i}/RT) \cdot dp_i/dx) \cdot \Phi \quad (4)$$

Where ρ is the density of zeolite, q_{sat} is the saturation amount adsorbed, $D^0(0)$ is intrinsic diffusivity which is independent of the amount adsorbed, θ is the fractional surface occupancy, E is the activation energy for diffusion, z is the probability factor, x is space coordinates, and Φ is the porosity size of a support.

Separation mechanism: In PV and VP on this study, separation factor >10000 suggests that activated gas translation diffusion can be disregarded in comparison with the surface diffusion.

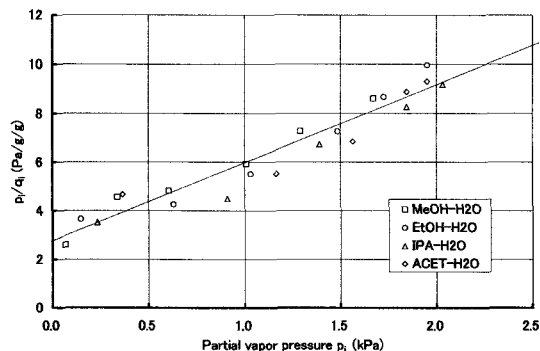


Fig. 5. Water adsorption data to NaA zeolite powder

The water adsorption data to NaA zeolite powder [12] is shown in Fig. 5, in which partial vapor pressure calculated by Wilson's equation and Antoine's equation from water content in organic solvent/water mixtures is used on the horizontal axis. These results suggest that the relation between the amount adsorbed and the partial vapor pressure can be displayed in the Langmuir type. By considering those results, Eq. 4 becomes Eq. 5.

$$J_{\text{total},i} = \varepsilon \cdot \rho \cdot D_i^0(0) \cdot \exp(-E_{s,i}/RT) \cdot q_{i,\text{sat}} \cdot b / (1 + b p_{i,1}) \cdot (p_{i,1} - p_{i,2}) / l \quad (5)$$

Where b is Langmuir adsorption parameter, l is the thickness of the zeolite membrane, and subscript 1, 2 are the feed and permeate side, respectively.

The water permeation in proportion to $p_{i,1}$ cannot be deduced from Eq. 5. We consider that water molecules are strongly adsorbed in the zeolite pores of the zeolite membrane, are carried to the non-zeolite pore by surface diffusion, and are condensed (or filled up) there. As a result, water molecules significantly inhibit the permeation of other molecules by blocking them from entering the non-zeolite pore.

Permeation mechanism: Water molecules collected in the non-zeolite pore are transported into the support by activated gaseous diffusion. We assume that the mass transfer of water molecules in non-zeolite pore decide permeation flux, because the adsorption rate of the zeolite is extremely rapid than diffusion velocity in the micro-pore and the crystals were randomly arranged. That is to say, the non-zeolite pore is playing an important role of the path that transports water molecule collected by the adsorption of the zeolite, as the following Eq. 6.

$$J_{\text{total},i} = \Phi \cdot \lambda / z \cdot \sqrt{8 / (\pi MRT)} \cdot \exp(-E_{GT,i}/RT) \cdot dp_i / dx \quad (6)$$

In this experiment range, the temperature dependency of $\lambda / z \cdot \sqrt{8 / (\pi MRT)} \cdot \exp(-E_{GT,i}/RT)$ in Eq. 6 seems to be very small, because the term is a function of \sqrt{T} . As the result, Eq. 6 is dependent on Φ and varies in proportion to $p_{i,1}$. These results suggest that the molecules absorbed by the zeolite fill easily non-zeolite pore of ca. 1.6 nm Kelvin diameter, and the number of this pore controls the permeation flux of the membrane.

4. CONCLUSION

(1) Average Kelvin diameters, which were defined as the diameters of nitrogen permeance of 50 %, were at ca. 1.8 nm Kelvin diameters regardless of the porosity size of the support. The maximum value of the pore size distribution of zeolite membranes was at ca. 1.6 nm Kelvin diameters regardless of the porosity size of the support, and only its value increased with the increase in the porosity size of the support.

(2) Regardless of the porosity size of the support, zeolite membranes were highly water permeable for IPA solution and displayed extremely high permeation fluxes and separations. The membrane performance in PV increased with the increase in the porosity size of the support. For industrial application of the membranes, the support with the porosity of 37.6 % was adopted from economic aspect. This membrane was ca. 1.2 times as high performance as the previous membrane.

(3) The high separation mechanism of PV and VP based on the capillary condensation (pore-filling) of water in the non-zeolite pore and the blocking of other molecules from entering the pore was proposed.

References

- [1] X.Feng and R.Y.M.Huang, *Ind. Eng. Chem. Res.*, 36, 1048 (1997).
- [2] Y.Morigami, M.Kondo, J.Abe, H.Kita and K.Okamoto, *Sep. Purif. Tech.*, 25, 251(2001).
- [3] M.Kondo, T.Yamamura, T.Yukitake, Y.Matsuo, H.Kita and K.Okamoto, *Sep. Purif. Tech.*, 32, 191(2003).
- [4] M.Kondo, M.Komori, H.Kita and K.Okamoto, *J. Membr. Sci.*, 133, 133(1997).
- [5] J.L.H.Chau, C.Tellez, K.L.Yeung and K.Ho, *J. Membr. Sci.*, 164, 257(2000).
- [6] T.Tsuru, T.Hino, T.Yoshioka and M.Asaeda, *J. Membr. Sci.*, 186, 257(2001).
- [7] H.Kita, K.Horii, Y.Ohtoshi, K.Tanaka and K.Okamoto, *J. Matr. Sci. Lett.*, 14, 206(1995).
- [8] K.Okamoto, H.Kita, M.Kondo, N.Miyake and Y.Mastuo, *US Pat.*, 5554286(1996).
- [9] K.Okamoto, H.Kita, K.Horii, K.Tanaka and M.Kondo, *Ind. Eng. Chem. Res.*, 40, 163(2001).
- [10] P.Huang, N.Xu, J.Shi and Y.S.Lin, *J. Membr. Sci.*, 116, 301(1996).
- [11] L.J.P.Broeke, W.J.Wbakker, F.Kapteijn and J.M.Moulijn, *AIChE J.*, 45, 976(1999).
- [12] M.Kondo, Y.Kumazawa, T.Yamamura, J.Abe, H.Kita and K.Okamoto, *MRS J.*, 29, 2591(2004).